

Open camera or QR reader and
scan code to access this article
and other resources online.



ORIGINAL ARTICLE

ALK-5 Inhibitors for Efficient Derivation of Mesenchymal Stem Cells from Human Embryonic Stem Cells

Shawn P. Grogan, PhD, Nicholas E. Glembotski, BS, and Darryl D. D'Lima, MD, PhD

Objectives: Successful tissue regeneration requires a clinically viable source of mesenchymal stem cells (MSCs). We explored activin receptor-like kinase (ALK)-5 inhibitors to rapidly derive an MSC-like phenotype with high cartilage forming capacity from a xeno-free human embryonic cell line.

Methods: Embryonic stem cell (ESC) lines (H9 and HADC100) were treated with the ALK-5 inhibitor SB431542; HADC100 cells were additionally treated with ALK-5 inhibitors SB525334 or GW788388. Cells were then seeded upon human fibronectin in the presence of fibroblast growth factor 2 (FGF2) in a serum-free medium. Flow cytometry was used to assess MSC markers (positive for CD73, CD90, and CD105; negative for CD34 and CD45). Differentiation status was assessed through quantitative polymerase chain reaction. Cartilage forming capacity was determined in high-density pellet cultures, in fibrin gels containing extracellular matrix (fibrin-ECM), and after implantation in *ex vivo* human osteoarthritic cartilage. Gene expression, histology, and immunostaining were used to assess cartilage phenotype, tissue regeneration, and integration.

Results: Exposure to all three ALK-5 inhibitors lead to expression of mesodermal gene markers and differentiation into MSC-like cells (embryonic stem cell-derived mesenchymal stem cells [ES-MSCs]) based on surface marker expression. ES-MSC in pellet cultures or in fibrin-ECM gels expressed high levels of chondrogenic genes: *COL2A1*, *ACAN*, and *COMP*; and low levels of *COL1A1* and *RUNX2*. Cell pellets or fibrin constructs implanted into *ex vivo* human osteoarthritic cartilage defects produced GAG-rich (safranin O positive) and collagen type II-positive neocartilage tissues that integrated well with native diseased tissue.

Conclusions: We developed a protocol for rapid differentiation of xeno-free ESC into MSC-like cells with high cartilage forming capacity with potential for clinical applications.

Keywords: embryonic stem cells, mesenchymal stem cells, ALK-5 inhibitor, stem cell differentiation, cartilage regeneration, cartilage repair

Impact Statement

Osteoarthritis (OA) is a common disease resulting in significant disability and no approved disease modifying treatment (other than total joint replacement). Embryonic stem cell-derived cell therapy has the potential to benefit patients with cartilage lesions leading to OA and may prevent or delay the need for total joint replacement.

Introduction

MESENCHYMAL STEM CELLS (MSCs) from several sources have been widely used as chondroprogenitors for cartilage regeneration.¹ Embryonic stem cell-derived mesenchymal stem cells (ES-MSCs) represent an attractive cell source for cartilage regeneration because of enhanced proliferative capacity and immunosuppressive properties in comparison with adult MSC in adipose tissue (ADSC) or MSC in bone marrow (BM-MSC).^{2–5} A variety of approaches have been used to generate MSC-like cells ranging from spontaneous differentiation to methods that specifically target certain pathways through sequential exposure to various molecules and culture conditions to recapitulate embryonic development.¹

Embryonic stem cells (ESCs) spontaneously differentiate when cultured on standard tissue culture plastic,⁶ or on Matrigel or gelatin coatings.^{7–9} We have previously demonstrated such spontaneous differentiation of H9 ESC on standard tissue culture plastic,⁶ through which the emergence of MSC-like cells increased with each subsequent passage with the capacity to form cartilage. An alternate approach involves initially directing ESC toward the primitive streak stage using a combination of molecules including activin A, BMP2, BMP4, fibroblast growth factor 2 (FGF2), Wnt3a, and CHIR99021 for a few days,^{10–16} followed by the addition of FGF2 and follistatin¹² or the inhibition of BMP receptors with dorsomorphin (DM) to induce paraxial mesoderm differentiation. Subsequent monolayer culture on various substrates promotes the emergence of an MEC-like phenotype. This approach recapitulates the complex stages of embryonic development and is a reproducible and well-characterized process to derive MSCs and chondroprogenitors.

Simpler and more targeted methods have been proposed that involve ALK-5 inhibitors^{17–19} or bromodomain-containing protein 4 (BRD4) inhibitors.²⁰ ALK-5 inhibitors block the ATP-binding domains of activin receptor-like kinase (ALK) receptors 4, 5, and 7 to inhibit SMAD 2/3 signaling and enhance SMAD 1/5/8 signaling.²¹ The decrease in SMAD2/3 phosphorylation reduces NANOG, SOX2, and OCT4 expression, alters methylation of OCT4 and NANOG,^{17,22} and induces ESC to differentiate.^{23,24} The increase in BMP4 expression directs ESC to a mesoderm fate.^{17,25} ALK-5 inhibitors have successfully induced an MSC-like phenotype in ESC.^{17–19}

One of the major issues limiting clinical translation of ES-MSC is the exposure to animal feeder cells or animal serum during culture or cryopreservation, which poses a risk of undesired xenogeneic contamination.^{26–29} Human-derived feeder cells, such as fetal fibroblasts, fetal muscle cells, adult dermal fibroblasts, and fallopian tubal epithelial cells, have been used to address this issue.^{30,31} Cell-free and xeno-free substrates have also been proposed including naturally derived extracellular matrices such as vitronectin, laminin, and fibronectin (FN) or synthetic substrates, such as PMVE-alt-MA, APMAAm, PMEDSAH, and PAM₆-co-PSS₂.^{32,33} Serum- and xeno-free reagents are also available for cell expansion and cryopreservation.^{34,35}

For safe clinical use, derivation of ES-MSC should be performed in completely xeno-free environments. Currently, there are several ESC lines that have been suc-

cessfully derived in xeno-free conditions.^{31,36–39} Xeno-free HADC100, 102, and 106 cell lines have been used for Phase I/II clinical trials for retinal degeneration and amyotrophic lateral sclerosis (clinicaltrials.gov).^{31,38} In 2018, four more clinical-grade xeno-free and feeder-free human ESC (hESC) lines (HADC 103, 104, 105, and 107) were made available.³⁸

To date, no clinical trials have been listed on clinicaltrials.gov using ESC-derived cells for cartilage tissue regeneration. Derivation of MSCs and chondroprogenitor cells under xeno-free conditions will reduce regulatory hurdles and may facilitate the use of hESC in clinical trials for cartilage regeneration. Toward this goal, we studied two ESC lines: the commonly studied ESC line (H9) and a xeno-free derived ESC line (HADC100). We compared the performance of ALK-5 inhibitors in directing MSC differentiation; assessed the chondrogenic performance of resultant ES-MSC; and evaluated the potential for cartilage repair in *ex vivo* arthritic human cartilage tissue. Our protocol for rapid and scalable differentiation of ESC to an MSC-like phenotype led to chondroprogenitors capable of robust neocartilage formation *in vitro* that integrated into *ex vivo* osteoarthritic tissue.

Methods and Materials

Cell sources

Two hESC lines (H9 and HADC100) were studied. The H9 ESC line was derived using irradiated mouse embryonic fibroblast feeder layers and cultured in fetal bovine serum, and has been extensively studied.^{5,8,15,25,40–42} We had previously characterized *in vitro* and *ex vivo* chondrogenic performance.⁶ This cell line is listed in the NIH registry as NIH-line WA 09 and was supplied by WiCell (Madison, WI) as the H9 line. The HADC100 ESC was derived by the Hadassah Medical Center as previously reported by Tannenbaum et al.³¹ Briefly, the HADC100 ESC line was developed in animal-free and good manufacturing practices-compliant culture system under clean room conditions. Donor eligibility was screened to follow regulatory guidelines. Each procedure from donor tissue and embryo handling, derivation of hESC, culturing, cryopreservation, characterization, and banking was monitored to satisfy quality practices for use in transplantation therapy. Human NUFF1 foreskin feeder cells were obtained from MTI-GlobalStem (Gaithersburg, MD).

ESC expansion

Thawed stocks of H9 ESC were seeded at a density of $1\text{--}1.5 \times 10^5$ cells/cm² on CELLstart (Thermo Fisher Scientific, Carlsbad, CA)-coated plates in StemPro hESC SFM medium (Thermo Fisher Scientific) with 8 ng/mL FGF2 (Thermo Fisher Scientific) and 10 μ M Y-27632 (EMD Millipore), with daily medium changes. H9 ESC were passaged by dissociation with Accutase[®] (Innovative Cell Technologies, Inc., San Diego, CA). Before cultivation of HADC100 ESC on CELLstart, the cells were defrosted and cultured on human foreskin feeders as previously described.³¹ To expand HADC100 ESC, a feeder cell layer was established by plating mitotically inactivated NUFF1 cells (NUFF1-MMC) onto gelatin (Stem Cell Technologies, Cambridge, MA)-coated

plates at a concentration of 30,000 cells/cm². Before seeding HADC100 ESCs, the feeder medium was changed to NutriStem hPSC XF (Biological Industries).

Thawed stocks of ESCs were seeded onto the NUFF1-MMC at a density between 10,000 and 13,000 cells/cm², with medium changes daily. HADC100 cells were passaged using TrypLE Select for 6 min and then seeded onto previously prepared NUFF1-MMC-seeded plates (24 h prior). For feeder-free cultures, HADC100 ESC were detached using TrypLE Select for 6 min and seeded on precoated CELLstart six-well plates in StemPro hESC SFM medium (Thermo

Fisher Scientific). For feeder-free expansion, the ESC were detached with Accutase and seeded upon the CELLstart substrate following the manufacturer's directions (Thermo Fisher Scientific) and using StemPro hESC SFM medium (Thermo Fisher Scientific).

ESC to MSC differentiation

An overview of the differentiation process is provided in Figure 1. To create cell clusters or embryoid bodies (EBs) of uniform size, ESC were removed from CELLstart culture

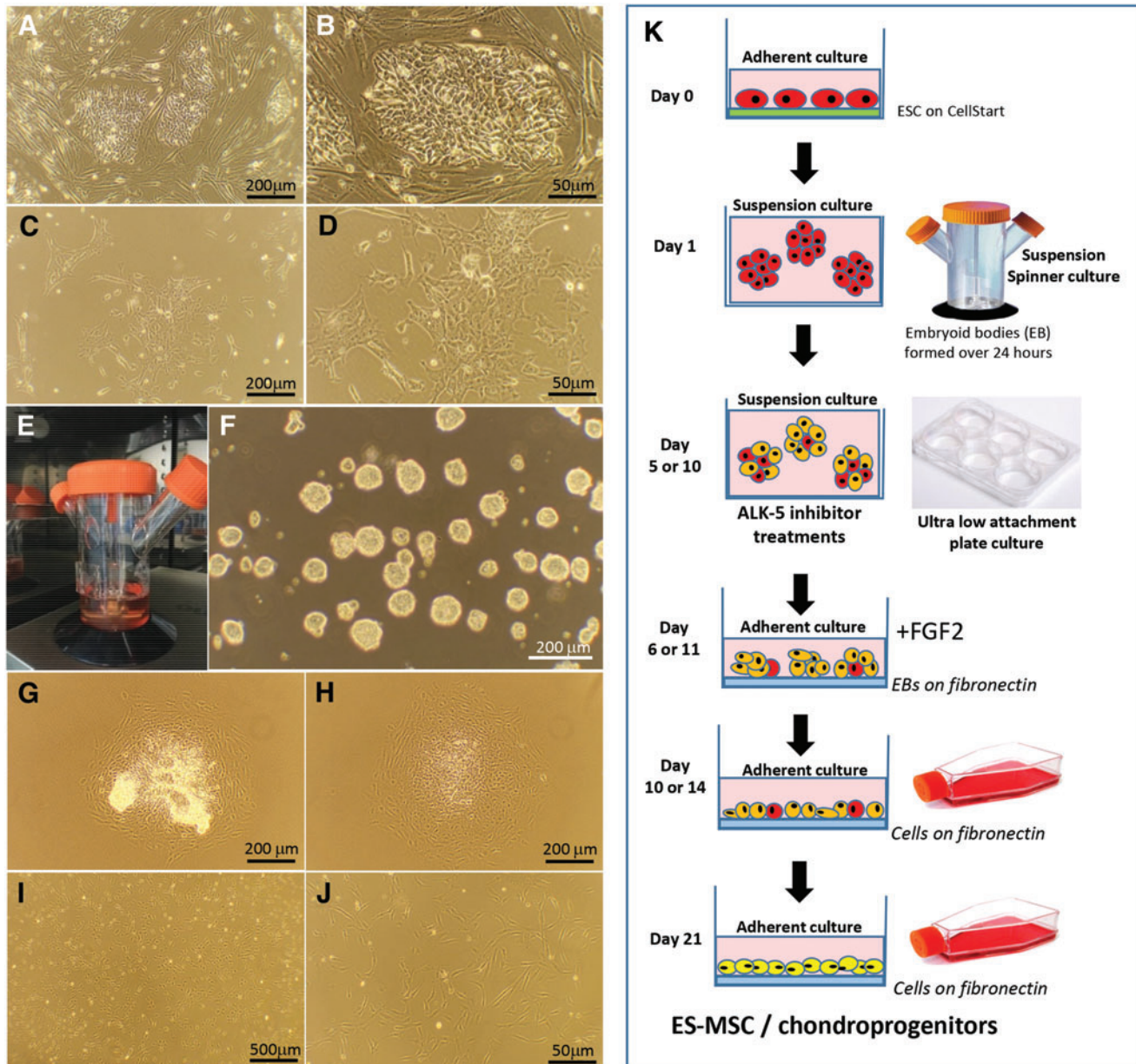


FIG. 1. Xeno-free approach to generate MSC-like cells from ESC. (A, B) ESC on human fibroblast feeders. (C, D) ESC on a cell-free substrate (CELLstart). (E) Spinner flask to generate cell clusters over 24 h. (F) Cell clusters following spinner culture ranged in size from 50 to 100 μm , with an average size of $75.8 \pm 17.7 \mu\text{m}$. (G, H) After 5–10 days of small-molecule exposure in low adherent plates, cell clusters seeded onto fibronectin-coated flasks to allow cell outgrowth for 4 days. (I, J) Typical morphology of ES-MSC-derived cells by day 21. (K) Overview of the differentiation process (see details in the Methods and Materials section). ESC, embryonic stem cell; ES-MSC, embryonic stem cell-derived mesenchymal stem cell; MSC, mesenchymal stem cell. Color images are available online.

using Accutase for 2–5 min until single cells were observed. Cells ($2.5\text{--}3 \times 10^5$ cells per mL) were suspended in StemPro hESC serum-free medium (Thermo Fisher Scientific) with $10\ \mu\text{M}$ Y-27632 (EMD Chemicals, Gibbstown, NJ) and $40\ \text{ng/mL}$ FGF2 (Life Technologies, Carlsbad, CA) in a 125 mL spinner culture flask (Corning, Inc., Corning, NY) on a magnetic stirrer (Cimarec™ Biosystem Slow-Speed Stirrer; Thermo Fisher Scientific) at 70 rpm for 24 h at 37°C with 5% CO_2 to form small cell clusters (minimum total cells were 7.5×10^6 in 30 mL).

After 24 h, the cell clusters were suspended at $2.5\text{--}3 \times 10^5$ cells per mL in ultralow adherent 6-well plates (Corning) in StemPro-34 serum-free medium (Thermo Fisher Scientific) supplemented with 2 mM L-glutamine (Thermo Fisher Scientific), 50 $\mu\text{g/mL}$ ascorbic acid (StemCell Technologies, Vancouver, Canada), and 1.8 $\mu\text{L/mL}$ ITS-G ($100 \times$ insulin–transferrin–selenium; Thermo Fisher Scientific); termed as “complete SP-34 medium.” For ESC to MSC differentiation, the complete SP-34 medium was supplemented with one of three ALK-5 inhibitors: SB431542 (SB43; $10\ \mu\text{M}$; Selleckchem, Houston, TX), or SB525334 (SB52; $10\ \mu\text{M}$; Selleckchem), or GW788388 (GW7; $5\ \mu\text{M}$; Selleckchem) or in 0.01% dimethyl sulfoxide (DMSO; Controls; Thermo Fisher Scientific) for 5 or 10 days. We explored a range of concentrations and times of exposure to ALK-5 inhibitors based on previous reports before selecting these conditions.^{17–19}

The medium was changed every 2 days by removing cell clusters into 15 mL sterile tubes and permitted to gravity settle for 10 min at room temperature. Most of the media were removed using a pipette to leave $\sim 300\text{--}500\ \mu\text{L}$ of medium. Freshly made medium (with the appropriate ALK-5 inhibitor or DMSO) was replaced at the same volumes and well number into new ultralow adherent plates.

After treatment with the appropriate ALK-5 inhibitor, the cell clusters were removed by gravity settling and suspended in complete SP-34 medium supplemented with FGF2 $20\ \text{ng/mL}$ (without any ALK-5 inhibitor or DMSO) and transferred onto FN-coated ($10\ \mu\text{g/mL}$; FN from human plasma; Sigma-Aldrich, St. Louis, MO) T75 cm^2 flasks. The cells were cultured for 4 days and considered as passage zero (P0). The emerging cells and remaining cell clusters were exposed to Accutase for 5–10 min, gently triturated, and counted. The cells were seeded at 4.5×10^5 per T75 cm^2 FN-coated flask (P1) and the medium changed every 3–4 days until 80–90% confluence. At this point, the cells were detached using Accutase for continued culture, screened for surface marker phenotype characterization (flow cytometry), placed into three-dimensional (3D) cultures to assess chondrogenic differentiation capacity, or preserved in liquid nitrogen.

Pellet cultures

Monolayer-expanded ES-MSCs (passage 2–5) were detached using Accutase, and 0.5×10^6 cells in 0.5 mL of chondrogenic medium were centrifuged at 900 rpm ($\sim 770\ g$) for 5 min to form high-density pellets. At least 5–6 pellets, for each ES-MSC condition, were cultured in serum-free chondrogenic medium consisting of Dulbecco’s modified Eagle’s medium (DMEM; Mediatech, Inc., Manassas, VA), $1 \times$ ITS supplement (Sigma-Aldrich), 100 nM dexamethasone (Sigma), 1.25 mg/mL human serum albumin (Bayer, Leverkusen, Germany), 100 μM ascorbic acid 2-phosphatate

(Sigma), 1% penicillin/streptomycin/gentamycin (PSG; Gibco, Carlsbad, CA), and 10 ng/mL TGF β 3 (PeproTech, Rocky Hill, NJ). Pellets for *ex vivo* implantation were cultured for 3 days before implantation; pellets for histologic or gene expression analysis were maintained in culture for 3 weeks with media changes every 2–3 days.

ESC hydrogel constructs

Monolayer cultured ES-MSCs were suspended in a hydrogel wafer composed of collagen II (Innovative Research, Inc., Novi, MI), hyaluronate (Supartz FX sodium hyaluronate; Seikagaku Corp., Tokyo, Japan), chondroitin sulfate (Sigma-Aldrich), and fibrin (Baxter Healthcare, Deerfield, IL) at a density of 20×10^6 cells per mL. The fibrinogen and thrombin components were prepared separately. To each fibrinogen component, 2 mg/mL of sodium hyaluronate, 2 mg/mL of chondroitin sulfate, and 6 mg/mL of collagen II were added ($2 \times$ concentration of final). Cells were added to the thrombin component at a density of 40×10^6 cells per mL. Thrombin and fibrinogen components in individual syringes were attached to a Baxter DUO mixing syringe and extruded to form the coagulation constructs.

The constructs were either directly implanted into *ex vivo* cartilage tissue or coagulated in six-well tissue-culture plates for 4–8 min before 4–6 mL of chondrogenic medium was added. To prevent shrinkage of the constructs during culture, the gels were held on AdminPatch microneedle arrays (AdminMed, Sunnyvale, CA) for the duration of their culture.

Ex vivo human osteoarthritic cartilage defect repair

Osteochondral tissues were obtained from patients ranging between 60 and 70 years of age undergoing total knee arthroplasty within 4–6 h of surgery (approved by Scripps Institutional Review Board) as previously described.⁴³ Cartilage disks (6 mm in diameter and $\sim 2\text{--}3$ mm thick) were harvested from the osteochondral specimens using a sterile dermal punch. The cartilage tissue was cultured in medium consisting of DMEM (Mediatech, Inc.) supplemented with 10% calf serum (Omega Scientific, Inc., Tarzana, CA) and 1% penicillin–streptomycin–gentamycin (Life Technologies). Cartilage disks were maintained in six-well plates (two to four per well) in 8 mL medium for 72 h before creation of the surgical defect. A flame-sterilized stainless-steel burr was used to create defects $\sim 2 \times 2$ mm wide and 0.5–1 mm deep. These defects were filled with pellets or hydrogel constructs trimmed to size using 2 mm dermal biopsy punches.

Gene expression profiling

Total RNA was extracted using the RNeasy kit as recommended by the manufacturer (QIAGEN, Valencia, CA). The High Capacity complementary DNA (cDNA) Reverse Transcription Kit (Applied Biosystems, Foster City, CA) was used to make cDNA and the following verified primer/probe assays were purchased from Applied Biosystems. Expression of the following genes was quantified: *POU5F1/OCT4* and *SOX2* (for pluripotency); *FOXA1* and *SOX17* (for endoderm); *NES* and *PAX6* (for ectoderm); *NKX2-5*, *MSX1*, *NCAM1*, and *SOX9* (for mesoderm); *ITGB1/CD29* (for MSC

phenotype); and *COL1A1*, *COL2A1*, *COL10A1*, *COMP*, *ACAN*, *SOX9*, and *RUNX2* (for chondrogenesis). Gene expression was normalized to *GAPDH* as previously reported.⁴⁴ Undifferentiated ESC served as a baseline for relative changes in gene expression in differentiated ES-MSC. Differentiated ES-MSC in monolayer served as a baseline for changes in gene expression in pellets or hydrogel constructs.

Flow cytometry

Cells were detached, washed, and suspended in FACS buffer at a concentration of 0.2×10^6 cells per 100 μ L. A panel of CD molecules were used, each with the following fluorochromes: CD34-FITC, CD45-BV510, and CD73-APC (BioLegend, San Diego, CA) and CD90-PE-Cy7 and CD105-BV650 (BD Biosciences, Franklin Lakes, NJ). Matching isotype control IgGs with the same fluorochrome conjugates were used for background gating. For compensation of spectral overlap, unstained cells and individual tubes with each fluorochrome were incubated with Dynabeads to distinguish between positive and negative fluorochrome signals. Data were acquired with the Novocyt flow cytometer (ACEA Biosciences, Inc., San Diego, CA) and analyzed using FlowJo software (version 10; FlowJo, LLC, Ashland, OR) to determine percentage positive signal for each molecule relative to isotype background nonspecific signal controls.

Histology and immunohistochemistry

Cell pellets and explants were fixed in Z-Fix (3.7% formaldehyde; Anatech Ltd., Battle Creek, MI), processed for embedding in paraffin, and cut into 4- μ m-thick sections. Sections were stained with safranin-O and fast green to visualize glycosaminoglycan distribution in the tissues. Alizarin red S staining was used to detect the presence of mineralized matrix.

For assessment of collagen types I and II, sections were pretreated with pepsin (Digest-All 3; Thermo Fisher Scientific) for 9 min at 37°C in a humid chamber before incubation at 4°C for 12–16 h with the following primary antibodies: rabbit anti-human collagen type I antibody (Ab 34710; Abcam, Cambridge, MA) 1 μ g/mL; or mouse anti-human collagen type II (II-II6B3; Hybridoma Bank, University of Iowa) 2 μ g/mL. For color development, the ImmPRESS secondary AP-red kit for collagen type I and DAB kit for collagen type II (Vector Laboratories, Burlingame, CA) were used. Isotype controls were used to monitor nonspecific staining.

Histology grading

Pellet cultures stained with safranin O were used for assessment of neocartilage quality using the Bern score as previously detailed.⁴⁵ Briefly, each section was assessed on the following three criteria: (1) safranin O staining profile, (2) the amount of extracellular matrix (ECM) formed, and (3) the cell morphologies represented. The score range is 0–9, with 9 being of the highest quality.

For assessment of cartilage repair in *ex vivo* OA tissue (implanted with either pellets or ES-MSC in fibro gel), we used an adapted Pineda grading approach.⁴⁶ The Pineda

grading system uses four criteria: (1) filling of defect (percentage), (2) reconstruction with osteochondral junction, (3) matrix staining, and (4) cell morphology. Since our *ex vivo* defects were chondral, we altered the second category to “integration with the surrounding chondral tissue.” The grading scores range from 0 to 14, with a score of 0 indicating the best cartilage regeneration score.

Histomorphometry image analysis was also performed on the same safranin O-stained pellets and *ex vivo* tissues. The images were quantified using ImageJ following a similar approach as detailed by Crowe and Yue.⁴⁷ Briefly, the color channels were separated using color deconvolution. For safranin O, the red channel was selected. The polygon tool was used to outline the pellet or *ex vivo* implant, respectively. A threshold was applied such that the empty space in the slide displayed no signal, thus ensuring that we were only measuring the signal that was distinguishable from background. On this thresholded image, a percent positive signal was recorded from the selected area.

Statistical analysis

Differences in flow cytometry surface markers between H9 and HAD cells were tested for significance using Student's *t*-test. Comparisons between individual surface markers for the different ALK-5 inhibitors and DMSO were tested using a single-factor analysis of variance and *post hoc* Bonferroni-corrected *t*-tests. Significant changes in gene expression between groups were analyzed using the online BootstRatio application, where *p*-values of <0.05 were considered significant.⁴⁸ Comparisons between histology scores for a given condition (DMSO and different ALK-5 inhibitors) were performed using the Student's *t*-test. Linear regression was used to test for correlations between the histology grading scores (Bern score and modified Pineda) and the histomorphometry data.

Results

Xeno-free culture expansion of ESC in suspension spinner-culture

HADC100 ESCs, defrosted and seeded initially upon mitotically inactivated human NUFF1 foreskin feeder cells, rapidly grew in distinctive clusters (Fig. 1A, B). H9 and HADC100 ESC, seeded upon a cell-free substrate of CELLstart, acquired a fibroblastic morphology (Fig. 1C, D). At ~80–90% confluence, the H9 or HADC100 ESC were detached using Accutase to achieve a near single-cell suspension and transferred to spinner culture flasks (Fig. 1E) for 24 h to produce cell clusters (Fig. 1F). Cell clusters were exposed to ALK-5 inhibitors for 5–10 days in ultralow adherent plates (5 days for SB52 and GW7, and 10 days for SB43). Cell clusters were then plated on human FN, without the presence of ALK-5 inhibitor and in the presence of FGF2; and cellular outgrowth was evident by 12–24 h (Fig. 1G, H).

After 4 days, the cells were detached and replated onto new FN-coated flasks until confluence. Representative morphology of expanded ES-MSC is shown in Figure 1I and J. No differences in cell morphology were observed among the different ALK-5 inhibitor treatments. An overview of the differentiation process is outlined in Figure 1K.

ALK-5 inhibition induces rapid differentiation to an MSC-like phenotype

HADC100 ESC, subjected to one of multiple ALK-5 inhibitors (SB43, SB52, or GW7), were compared with H9 ES-MSC (subjected to SB43) and a DMSO control. Following exposure to each single ALK-5 inhibitor, subsequent adherent culture, and mesoderm differentiation, both H9 ESC and HADC100 ESC showed a significant loss of pluripotent markers *POU5F1* (*OCT4*) and *SOX2* (Supplementary Fig. S1). To assess cytotoxicity, we compared the morphology and proliferation of cells exposed to ALK-5 inhibitors relative to DMSO controls. We did not find changes in morphologies and capacity to grow in the doses used in our study. Our results are also consistent with previous reports that treatment with ALK-5 inhibitors reduced TGF β 1-mediated cell death.^{49,50}

The expression of endoderm markers (*SOX17*, *FOXA1*, and *PAX6*) remained low in ESC and ES-MSC, and the

ectoderm marker (*NES*) expression was unchanged by treatment (Supplementary Fig. S1). On the contrary, mesoderm-specific markers (*NCAM1*, *MSX1*, and *NKX2-5*) and MSC marker (*ITGB1*) were significantly upregulated. Increased expression of *SOX9* and *COL2A1* indicated a chondroprogenitor phenotype (Fig. 2). Treatment of the HADC100 ESC with DMSO (control) resulted in spontaneous differentiation toward a mesoderm phenotype (Fig. 2), without specifically inducing a chondroprogenitor phenotype (*COL2A1*).

H9 ESC ($N=5$) and HADC100 ESC ($N=4$) were differentiated to ES-MSC using SB43 (10 μ M) for 10 days for a direct comparison between the two cell lines. A surface marker profile resembling an MSC phenotype was observed (positive for CD73, CD90, and CD105; and negative for hematopoietic markers CD34 and CD45) (Fig. 3 and Supplementary Fig. S2).⁵¹ H9 ES-MSC displayed significantly ($p < 0.04$) higher percentage levels of CD90 (99% \pm 1%) and CD105 (94% \pm 4%) compared with the HADC100 ES-MSC

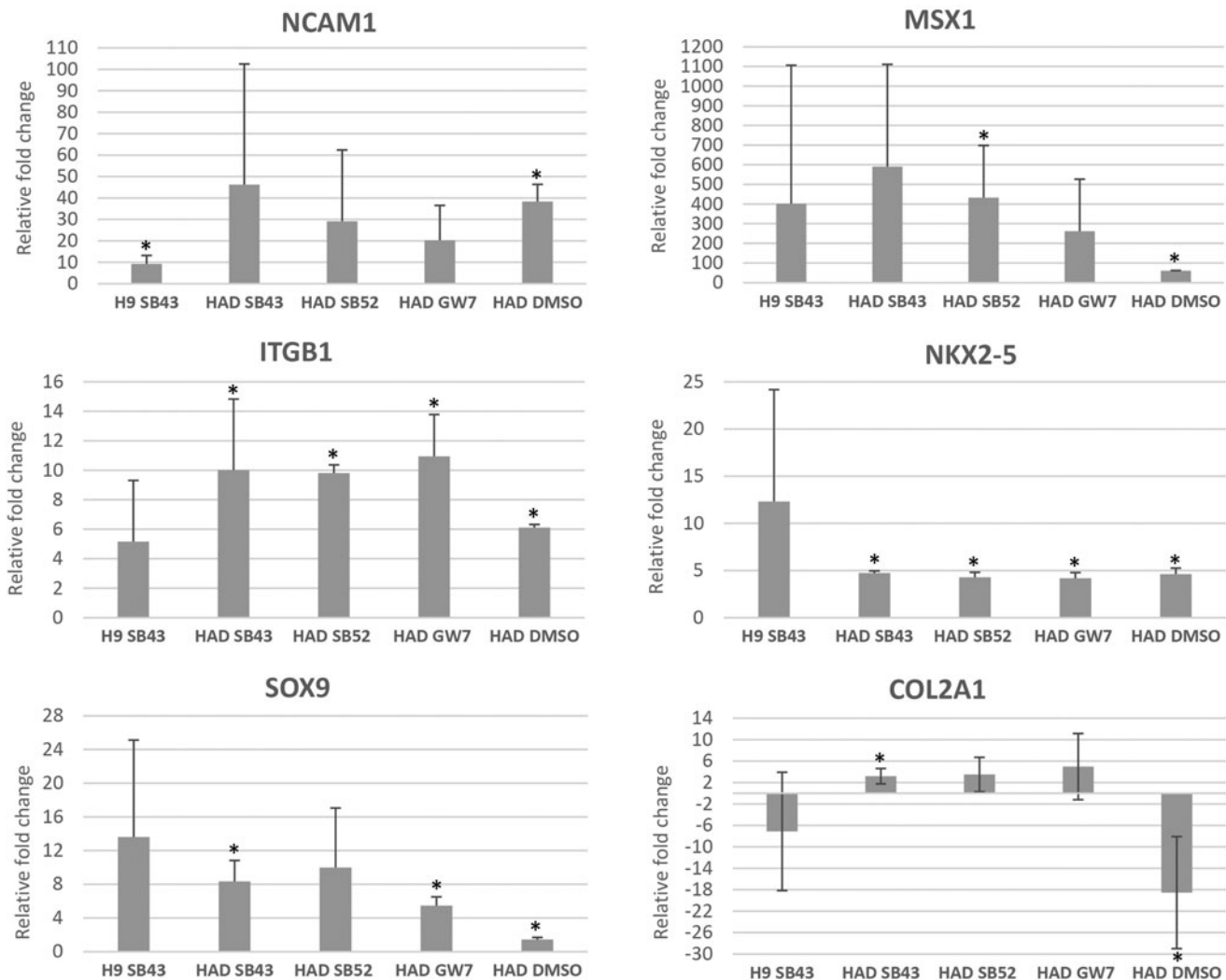


FIG. 2. Mesoderm, MSC, and chondrogenic gene expression levels (mean \pm SD) relative to the matching undifferentiated ESC type ($N=3-4$). * $p < 0.05$ compared with undifferentiated ESC. H9 SB43 and H9-ES-MSC treated with SB431542; HAD SB43 and HADC100-ES-MSC treated with SB431542; HAD SB52 and HADC100-ES-MSC treated with SB525334; HAD GW7 and HADC100-ES-MSC treated with GW788388; HAD DMSO and HADC100-ES-MSC treated with DMSO (control). DMSO, dimethyl sulfoxide; SD, standard deviation.

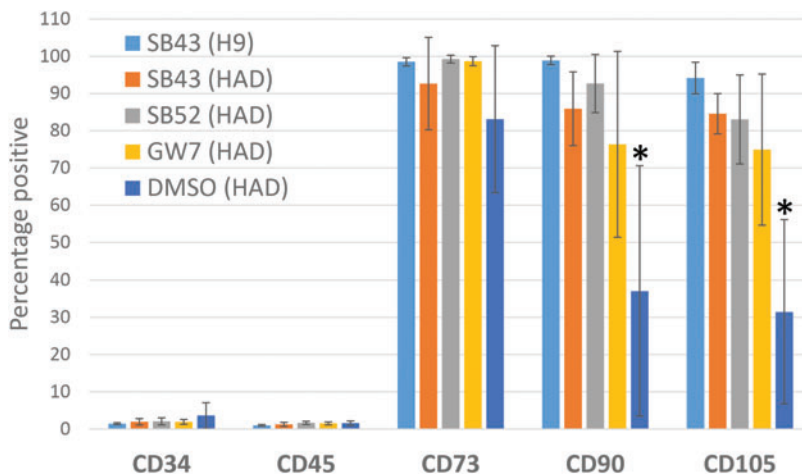


FIG. 3. Flow cytometric evaluations for MSC surface markers (mean \pm SD percentage positive signal) for comparison of cells following treatment of H9 ESC with SB43 or HADC100 ESC with three different ALK-5 inhibitors and DMSO ($N=4-5$). Surface marker expression levels of CD90 and CD105 significantly lower than all other ES-MSC treatments ($*p < 0.05$). ALK, activin receptor-like kinase. Color images are available online.

(CD90: $88\% \pm 10\%$ and CD105: $86\% \pm 7\%$). No significant difference for CD73 (H9: $99\% \pm 1\%$ and HAD: $94\% \pm 12\%$) was observed between these two ES-MSC-derived cells (Fig. 3). Coexpression analysis revealed that the H9-ES-MSC was $92\% \pm 9\%$ triple positive for CD73, CD90, and CD105; HADC100 ES-MSC was $88\% \pm 8\%$ triple positive (not significantly different).

We compared alternative ALK-5 inhibitors SB52 ($10 \mu\text{M}$) or GW7 ($5 \mu\text{M}$) with SB43 ($10 \mu\text{M}$) for derivation of ES-MSC from xeno-free HADC100 ESC ($N=4$ each condition) (Fig. 3 and Supplementary Table S1). The concentrations and duration of exposure were based on initial evaluations. CD73 was highly expressed by all cell treatments (SB43: $93.6\% \pm 11.8\%$; SB52: $99.2\% \pm 1.0\%$; GW7: $98.9\% \pm 1.1\%$), including DMSO controls ($83.1\% \pm 19.7\%$), with no significant differences between treatments (Fig. 3). A significantly higher expression of CD90 and CD105 was seen in the SB43 (CD90: 87.6 ± 10.4 ; CD105: 86.1 ± 6.5), SB52 (CD90: 93.9 ± 7.6 ; CD105: 85.4 ± 12.2), and GW7 (CD90: 80.9 ± 23.9 ; CD105: 79.6 ± 20.5) treatments compared with the DMSO control (CD90: 37.1 ± 33.5 ; CD105: 31.4 ± 24.7) ($p < 0.05$; Fig. 3).

There were no significant differences for these surface molecules among the three ALK-5 inhibitor treatments tested. As stated earlier, SB43-treated HAD-ES-MSCs were observed to be $88\% \pm 8\%$ triple positive, while SB52-treated ES-MSCs were $87\% \pm 8\%$ triple positive; GW7-treated cells were $78\% \pm 13\%$; and DMSO controls $44\% \pm 31\%$ triple positive (for CD73, CD90, and CD105).

Cell pellets synthesize cartilaginous matrix and integrate into *ex vivo* osteoarthritic cartilage

Chondrogenesis in high-density pellets of ES-MSC (H9 after SB43 treatment and HADC100 after SB43, SB52, or GW7 treatment) was assessed after 3 weeks (Figs. 4 and 5). Both cell lines (after SB43 treatment) consistently produced cartilage like-tissue with extensive ECM staining strongly with safranin-O and evidence of collagen type II, and low collagen type I deposition. HAD ES-MSC generated with exposure to 2 alternative ALK-5 inhibitors (SB52 and GW7) also produced cartilage-like tissue. SB52-treated cells showed the most consistent staining for GAGs

and collagen type II, and lower collagen type I signal compared with SB43 and GW7. Control (DMSO)-treated cells displayed no positive signal for GAGs or collagen type II (Fig. 5A). Histology grading of safranin O-stained pellets revealed that all conditions produced significantly better quality neocartilage tissues in comparison with the DMSO controls ($p < 0.005$) (Supplementary Fig. S3A).

The cartilage quality of pellet cultures produced by SB52-treated HAD ES-MSC was significantly better than HAD ES-MSC derived from SB43 treatments ($p < 0.02$), which is consistent with the better staining profiles of collagen type I (low) and type II (high and more uniform). We also tested the ES-MSC incubated as pellet cultures and implanted in *ex vivo* explants of human osteoarthritic cartilage as previously described.^{6,43} Both H9 and HADC100 ES-MSC pellets generated robust cartilage-like tissue (rich in GAGs and collagen type II) that integrated well with the diseased host tissue (Figs. 4M–R and 5B). Histological grading of *ex vivo* implantations of pellets was similar to the Bern score data where all *ex vivo* tissues implanted with DMSO-treated ES-MSC were graded a significantly ($p < 0.02$) higher score (lower quality) using the adapted Pineda grading system (Supplementary Fig. S3B).

Histomorphometry data (image analysis) also confirmed the histology grading scores. Linear regression analyses between the image analysis (percentage positive for red) and both Bern and adapted Pineda scores show these methods to be highly correlated ($p < 0.0001$) (Supplementary Fig. S3C, D).

Chondrogenic gene expression was compared between ES-MSCs derived from H9 ESC or HADC100 following exposure to SB43. Pellets from either ES-MSC source expressed higher levels of chondrogenic genes (*COL2A1*, *ACAN*, *COMP*, and *SOX9*) relative to their respective monolayer controls (Fig. 6). No significant differences were noted between H9 and HAD ES-MSC for *COL1A1* and *COL2A1* expression. However, significantly higher *ACAN* ($p = 0.003$), *COMP* ($p = 0.04$), and *SOX9* ($p = 0.006$) were observed in H9 ES-MSC compared with HAD ES-MSC. H9 ES-MSC also expressed higher levels of the hypertrophic marker, *COL10A1* ($p = 0.03$), and osteogenic transcription factor *RUNX2* ($p = 0.007$).

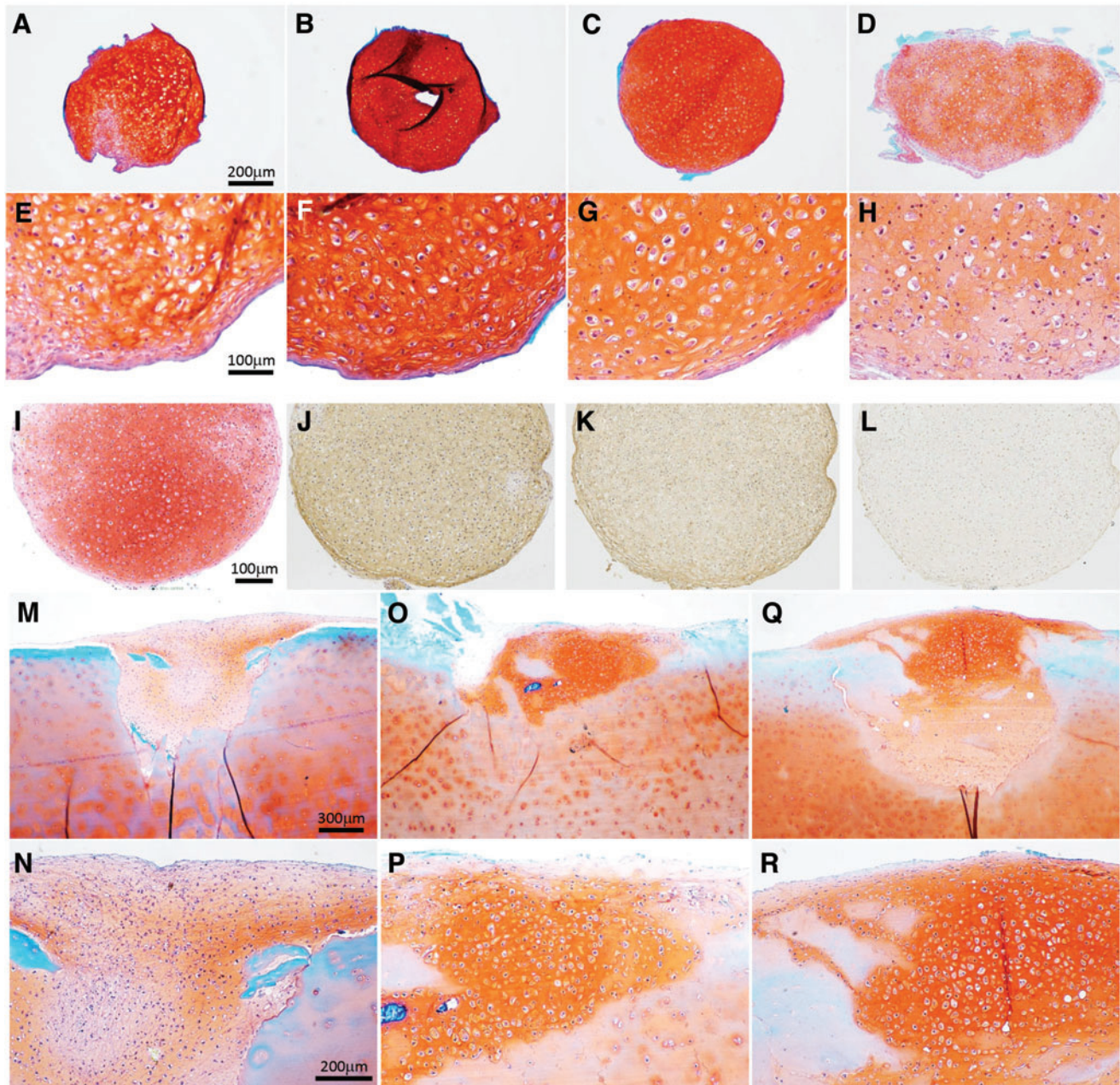


FIG. 4. Chondrogenic differentiation of H9-derived ES-MSC. (A–H) Safranin O fast green-stained 3-week cultured pellets from four different differentiations. (I) Safranin O fast green-stained 3-week cultured pellet. (J) Collagen type II immunostained pellet. (K) Collagen type I immunostained pellet. (L) Isotype control staining. (M–R) Safranin O fast green staining of pellets implanted in *ex vivo* human OA cartilage and cultured for 3 weeks. OA, osteoarthritis. Color images are available online.

ES-MSCs embedded in fibrin gels containing ECM hydrogels create neocartilage tissues and integrate in ex vivo OA tissue

To enable surgical delivery of cells and to facilitate shaping and implantation into chondral or osteochondral lesions, we developed a fibrin hydrogel supplemented with the major ECM components of articular cartilage: collagen type II, hyaluronate, and chondroitin sulfate (fibrin gels containing extracellular matrix [fibrin-ECM]). HAD ES-MSCs differentiated with SB43 were mixed in the hydrogel

at a density of 20×10^6 cells per mL and mounted upon several needle arrays ($N=8$) to maintain size and shape during culture (Fig. 7A). After 3 weeks of culture, a mechanically stable construct was formed on the needle array (Fig. 7A) with production of cartilaginous tissue (safranin O fast green staining; Fig. 7B, C). The gene expression profile of these neotissues was chondrogenic (Fig. 7D) and resembled that of the pellet cultures from the same cell source (Fig. 6).

For comparison among ALK-5 inhibitors, ES-MSCs differentiated with SB43, SB52, or GW7 treatment, and

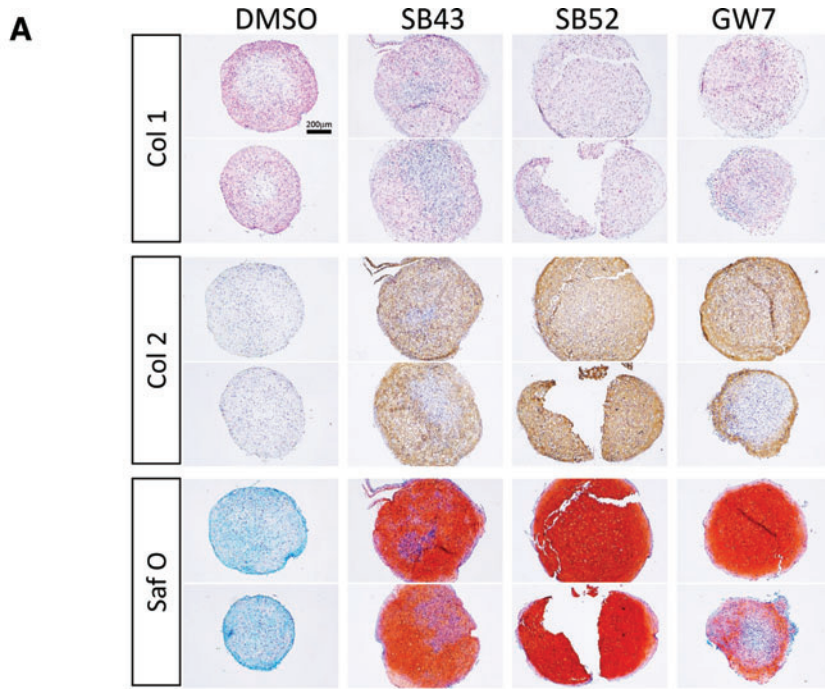


FIG. 5. Pellet culture and *ex vivo* implantation of HADC100-derived ES-MSCs differentiated with different ALK-5 inhibitors. **(A)** Histology of pellets derived from DMSO (control), SB431542 (SB43), SB525334 (SB52), or GW788388 (GW7). Pellets were immunostained for collagen type I (AP-red), collagen type II (DAB), or stained with safranin O fast green. **(B)** Histology of various pellets implanted into osteoarthritic *ex vivo* tissues ($N=3-4$). Color images are available online.

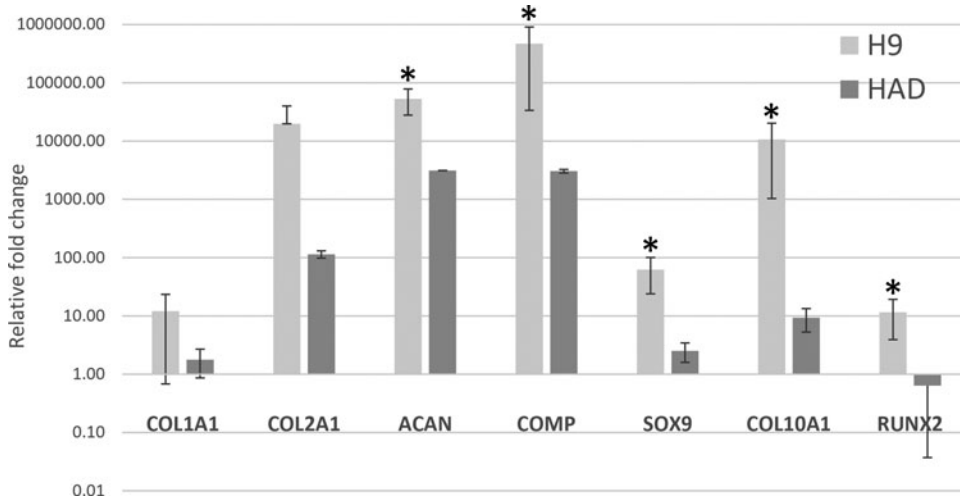
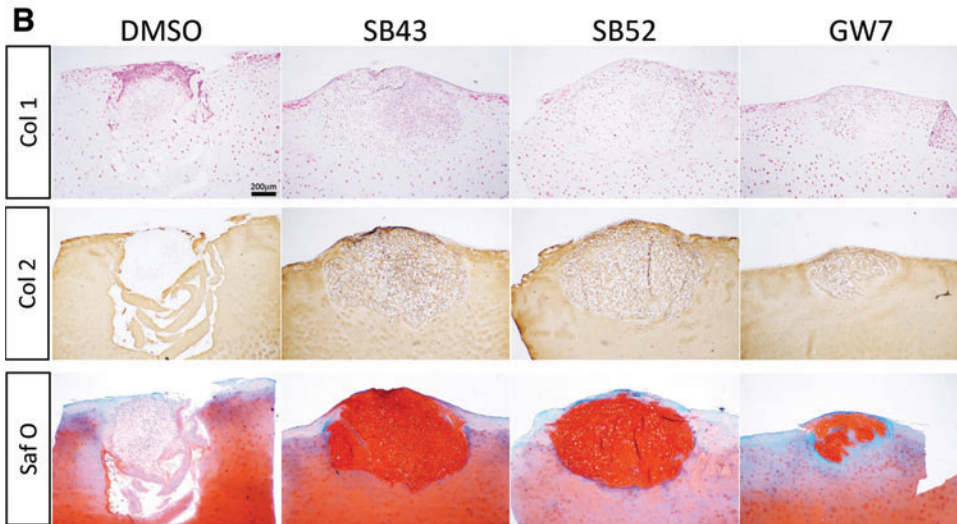


FIG. 6. A direct comparison between the relative gene expression profiles (mean \pm SD) of pellet cultured cells derived from either H9-ES-MSC (H9) or HADC100 ES-MSC (HAD) and differentiation using SB431542 treatment ($*p < 0.04$). Gene expression levels are relative to undifferentiated monolayer cultured ES-MSCs.

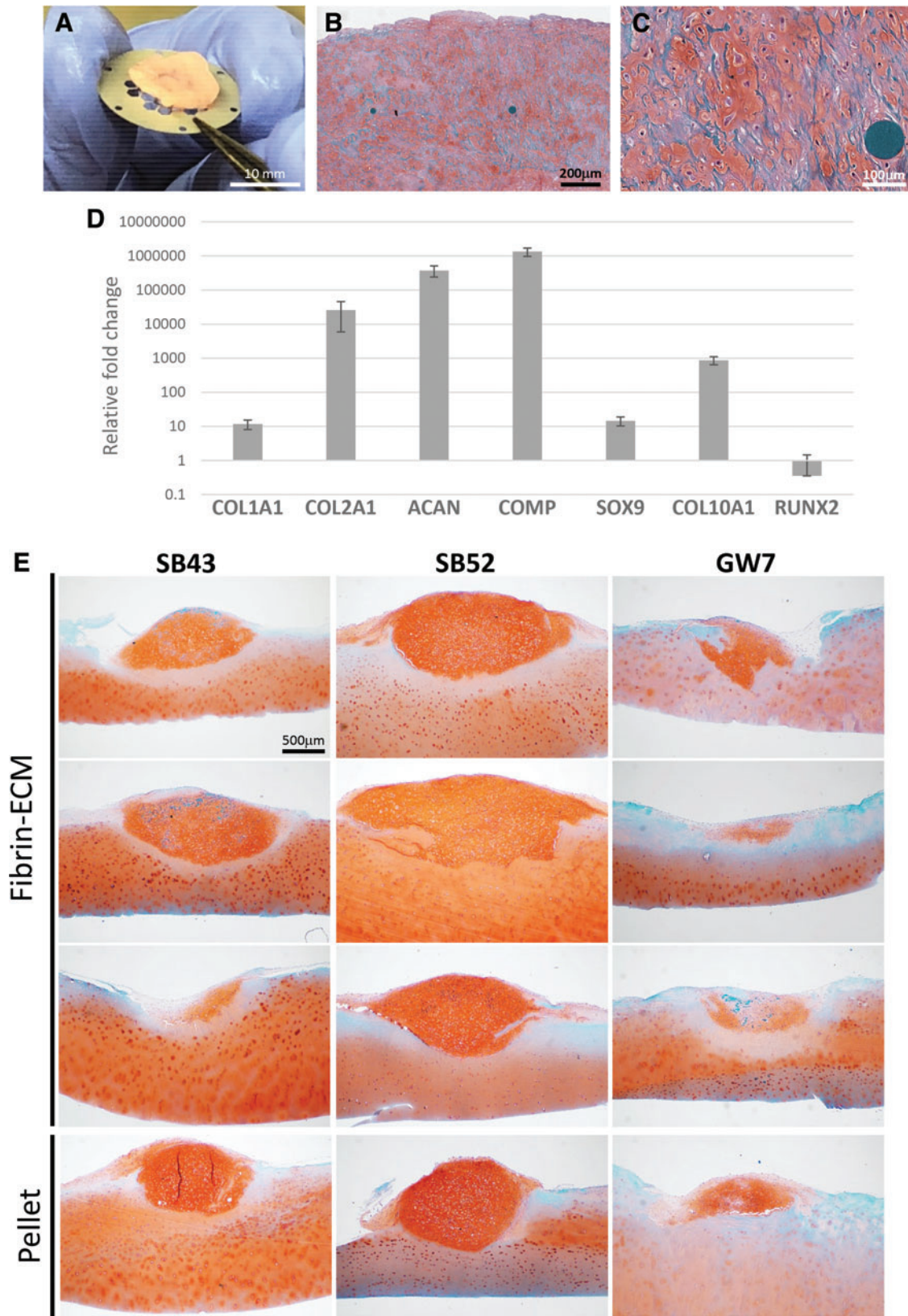


FIG. 7. Creation of implantable constructs with ECM-fibrin hydrogels. **(A)** After 3 weeks on a needle array using HAD-MSC (SB43 treatment). **(B, C)** Safranin O staining of 3-week-old cultured fibrin-ECM constructs. **(D)** Gene expression profile (mean \pm SD) of several fibrin-ECM constructs relative to the undifferentiated monolayer ES-MSC ($N=8$). **(E)** Safranin O staining of *ex vivo* OA cartilage explants with either fibrin-ECM or pellets using HAD-MSCs derived by three different ALK-5 inhibitor treatments. Fibrin-ECM, fibrin gels containing extracellular matrix. Color images are available online.

suspended in fibrin-ECM constructs were immediately implanted into defects created in *ex vivo* osteoarthritic cartilage explants. For comparison, pellet cultures from the same cell sources were also implanted into osteoarthritic explants, in parallel experiments. Following 3 weeks in serum-free chondrogenic medium with TGF β 3 (10 ng/mL), cartilaginous neo-tissues formed equally well in all ALK-5 inhibitor conditions, implanted as hydrogel or pellets (Fig. 7E). Histology grading of these fibro gel *ex vivo* cultures also showed consistently high-quality cartilage tissue formation (Supplementary Fig. S3B).

Hypertrophic differentiation is a major concern in adult BM-ESC.⁵² Because H9-ES-ESC expressed higher levels of *COL10A1* and *RUNX2* (Fig. 6), we examined hypertrophic differentiation and mineralization in the neotissues generated from both H9-ES-ESC and HAD-ES-ESC through alizarin red S staining. No evidence of mineralization was observed for any cell line studied in pellet culture or in fibrin-ECM hydrogels in free culture or after *ex vivo* implantation (Supplementary Fig. S4).

Discussion

We developed a rapid and simple approach to derive ES-ESCs, with high chondrogenic capacity, from the commonly studied H9 ESC line and a clinically relevant xeno-free derived HADC100 cell line. Overall, both ESC lines responded equivalently to the small-molecule differentiation approach used in this study. ALK-5 inhibitors (particularly SB52) successfully induced MSC differentiation in HADC100 cells. ES-ESCs from H9 and HADC100 cells produced high-quality neocartilage tissues with robust deposition of GAGs and collagen type II, without evidence of mineralization, as pellets in free culture, when encapsulated in ECM-fibrin hydrogel, as well as after implantation into osteoarthritic *ex vivo* tissue.

We had previously reported on our approach to spontaneously derive chondroprogenitors from H9-ESC.⁶ This approach was relatively simpler than other spontaneous differentiation approaches using Matrigel⁷ or gelatin^{8,9} and consecutive enzymatic passaging. However, Olee et al⁶ expanded ESC on mouse embryonal fibroblast feeders and ESC differentiation required relatively longer culture times (up to five passages) for the consistent emergence of an MSC phenotype. In the present study, after expanding H9-ESC without mouse feeders and subsequently culturing on FN-coated flasks, we derived chondroprogenitor cells at a lower passage (P1–P2). We then reproduced our results in the xeno-free HADC100 ESC line, initially cultured on human foreskin feeder cells, under otherwise identical differentiation conditions.

ALK-inhibitors have been shown to induce MSC differentiation in various pluripotent lines, under different culture substrates and techniques.¹ Mahmood et al suspended HUES9 ESC EBs in 10 μ M SB43 before plating on FN to induce emergence of fibroblastic cells, which were subsequently cultured in monolayer with 10% FBS and continued exposure to SB43.¹⁸ The resultant cells were highly enriched for MSC markers CD44, CD73, CD146, and CD166, although CD90 and CD105 were not reported. Sánchez et al exposed several ESC lines (H9, AND-1, AND-2, and SHEF-1) to SB43 in monolayer cultures on Matrigel-coated flasks.¹⁹ This approach led to a fibroblastic cell population

that was only 42% CD73⁺CD90⁺CD34⁻ (comparable with our results with DMSO-negative controls), and subsequent sorting for CD73 and CD90 double-positive cells was required to increase purity to >85%.

Chen et al¹⁷ differentiated Mel1 and HES3 ESC lines. The cells cultured in monolayer on Matrigel initially acquired an epithelial-like morphology, eventually differentiating into an MSC-like phenotype upon subsequent culture. Cells cultured as EBs after 10 days of SB43 treatment and subsequently seeded on standard tissue culture plastic gave rise to a heterogeneous population of cells, with MSC-like surface markers, and the capacity to undergo osteogenesis and chondrogenesis. In general, our method of differentiation was more efficient, did not require xeno-derived reagents (such as Matrigel), and performed equivalently with xeno-free derived HADC100 ESC.

Although SB43 is one of the most commonly used ALK-5 inhibitors, we explored the efficacy of two other ALK-5 inhibitors. SB43 and SB52 appear to be equally effective in differentiating ES-ESC. SB43 seemed superior in terms of generating mesoderm markers (such as NCAM1 and SOX9) and increasing the expression of *COL2A1* as ES-ESC in monolayer culture. On the contrary, SB52-treated cells developed neocartilage tissues with the most uniform GAGs and collagen type II deposition, with reduced collagen type I and significantly better histology grades (pellet cultures). While these small-molecule ALK-5 inhibitors are promising, there may be concerns about the use of ALK-5 inhibitors for clinical applications. However, several ALK-5 inhibitors are in clinical trials for various therapies (see Abdel Mouti and Pauklin,⁵³ Herbertz et al,⁵⁴ Kim et al,⁵⁵ and Wang et al⁵⁶). Therefore, the transient (5–10 days) exposure to cells is less likely to be an issue for tissue engineering cell therapy.

Other small molecules are being explored to produce chondroprogenitors from human pluripotent cells. CHIR99021, a glycogen synthase kinase 3 inhibitor, and TTNPB, a retinoid acid receptor agonist, have been used to produce chondroprogenitors from human induced pluripotent stem cells.⁵⁷ This simple protocol led to sequential differentiation through the mesendoderm and mesoderm, and to chondroprogenitors, leading to abundant collagen type II immunocytochemical staining.⁵⁷ However, the pluripotent cells had been cultured on mouse embryonic fibroblast feeders. BRD4 interacts with OCT4 and pluripotency genes, augments histone acetylation, maintains the expression and chromatin patterns of pluripotency-associated genes, and controls the master regulators of mesoderm formation including brachyury.^{58,59} Combining BRD4 inhibitors (LLY-507 and AZD5153) successfully induced MSC phenotype in pluripotent stem cells after monolayer culture on Matrigel-coated plates, with subsequent culture in MSC culture medium.²⁰

We only tested two ESC lines, and other cell lines may perform differently. In this study, we focused on cartilage formation, which is our primary translational target. We are exploring the potential for ES-ESC to undergo osteogenic differentiation for potential use in bone regeneration. The performance of ES-ESC for other musculoskeletal tissues might be different. In addition to xenogeneic issues, there are safety concerns universally related to ESC-derived cells that include off-target biodistribution of implanted cells,

teratogenic potential, and allogeneic responses. Our results of promising tissue regeneration in arthritic *ex vivo* cartilage will require preclinical validation *in vivo* for effective translation.

We demonstrated the feasibility of rapidly deriving ES-MSCs and chondroprogenitors with high cartilage forming capacity using the commonly studied H9 ESC line and a more clinically relevant xeno-free derived ESC line. The derived ES-MSCs were able to produce high-quality neo-cartilage tissues with robust deposition of GAGs and collagen type II, as pellets in free culture, when encapsulated in ECM-fibrin hydrogel, and after implantation into osteoarthritic *ex vivo* tissue. Further testing *in vivo* is needed to evaluate the suitability of ES-MSC lines for clinical applications.

Acknowledgments

We thank April Damon for technical assistance with quantitative polymerase chain reaction (qPCR), histology, and immunostaining. We are also grateful to Erik Dorthé for technical assistance with the histomorphometry analysis.

Authors' Contributions

S.P.G. and D.D.D. were responsible for the overall experimental design. S.P.G. and D.D.D. wrote the article in close collaboration with the other authors. N.E.G. maintained and cultured the ESC. S.P.G. performed the differentiations. S.P.G. and N.E.G. performed the flow cytometry, 3D cultures, and *ex vivo* studies. S.P.G. coordinated or performed qPCR characterizations. All authors discussed the results and approved the final version of the article.

Disclosure Statement

No competing financial interests exist.

Funding Information

This work was funded by CIRM (PC1-08128); the Shaffer Family Foundation; and Donald and Darlene Shiley.

Supplementary Material

Supplementary Figure S1
Supplementary Figure S2
Supplementary Figure S3
Supplementary Figure S4
Supplementary Table S1

References

- Grogan SP, Kopkow J, D'Lima DD. Challenges facing the translation of embryonic stem cell therapy for the treatment of cartilage lesions. *Stem Cells Transl Med* 2022;11(12):1186–1195; doi: 10.1093/stcltm/szac078
- Brown PT, Squire MW, Li WJ. Characterization and evaluation of mesenchymal stem cells derived from human embryonic stem cells and bone marrow. *Cell Tissue Res* 2014;358(1):149–164.
- de Peppo GM, Svensson S, Lenneras M, et al. Human embryonic mesodermal progenitors highly resemble human mesenchymal stem cells and display high potential for tissue engineering applications. *Tissue Eng Part A* 2010;16(7):2161–2182.
- Trivedi P, Hematti P. Derivation and immunological characterization of mesenchymal stromal cells from human embryonic stem cells. *Exp Hematol* 2008;36(3):350–359.
- Vodyanik MA, Yu J, Zhang X, et al. A mesoderm-derived precursor for mesenchymal stem and endothelial cells. *Cell Stem Cell* 2010;7(6):718–729.
- Olee T, Grogan SP, Lotz MK, et al. Repair of cartilage defects in arthritic tissue with differentiated human embryonic stem cells. *Tissue Eng Part A* 2014;20(3–4):683–692.
- Lee PT, Li WJ. Chondrogenesis of embryonic stem cell-derived mesenchymal stem cells induced by TGFbeta1 and BMP7 through increased TGFbeta receptor expression and endogenous TGFbeta1 production. *J Cell Biochem* 2017;118(1):172–181.
- Nakagawa T, Lee SY, Reddi AH. Induction of chondrogenesis from human embryonic stem cells without embryoid body formation by bone morphogenetic protein 7 and transforming growth factor beta1. *Arthritis Rheum* 2009;60(12):3686–3692.
- Karlsson C, Emanuelsson K, Wessberg F, et al. Human embryonic stem cell-derived mesenchymal progenitors—Potential in regenerative medicine. *Stem Cell Res* 2009;3(1):39–50.
- Cheng A, Kapacee Z, Peng J, et al. Cartilage repair using human embryonic stem cell-derived chondroprogenitors. *Stem Cells Transl Med* 2014;3(11):1287–1294.
- Craft AM, Rockel JS, Nartiss Y, et al. Generation of articular chondrocytes from human pluripotent stem cells. *Nat Biotechnol* 2015;33(6):638–645.
- Oldershaw RA, Baxter MA, Lowe ET, et al. Directed differentiation of human embryonic stem cells toward chondrocytes. *Nat Biotechnol* 2010;28(11):1187–1194.
- Wang T, Nimkingratana P, Smith CA, et al. Enhanced chondrogenesis from human embryonic stem cells. *Stem Cell Res* 2019;39:101497.
- Wu CL, Dicks A, Steward N, et al. Single cell transcriptomic analysis of human pluripotent stem cell chondrogenesis. *Nat Commun* 2021;12(1):362.
- Evseenko D, Zhu Y, Schenke-Layland K, et al. Mapping the first stages of mesoderm commitment during differentiation of human embryonic stem cells. *Proc Natl Acad Sci U S A* 2010;107(31):13742–13747.
- Wu L, Bluguermann C, Kyupelyan L, et al. Human developmental chondrogenesis as a basis for engineering chondrocytes from pluripotent stem cells. *Stem Cell Reports* 2013;1(6):575–589.
- Chen YS, Pelekanos RA, Ellis RL, et al. Small molecule mesengenic induction of human induced pluripotent stem cells to generate mesenchymal stem/stromal cells. *Stem Cells Transl Med* 2012;1(2):83–95.
- Mahmood A, Harkness L, Schroder HD, et al. Enhanced differentiation of human embryonic stem cells to mesenchymal progenitors by inhibition of TGF-beta/activin/nodal signaling using SB-431542. *J Bone Miner Res* 2010;25(6):1216–1233.
- Sánchez L, Gutierrez-Aranda I, Ligerio G, et al. Enrichment of human ESC-derived multipotent mesenchymal stem cells with immunosuppressive and anti-inflammatory properties capable to protect against experimental inflammatory bowel disease. *Stem Cells* 2011;29(2):251–262.

20. Zhang L, Wei Y, Chi Y, et al. Two-step generation of mesenchymal stem/stromal cells from human pluripotent stem cells with reinforced efficacy upon osteoarthritis rabbits by HA hydrogel. *Cell Biosci* 2021;11(1):6.
21. Du J, Wu Y, Ai Z, et al. Mechanism of SB431542 in inhibiting mouse embryonic stem cell differentiation. *Cell Signal* 2014;26(10):2107–2116.
22. Samadian A, Hesaraki M, Mollamohammadi S, et al. Temporal gene expression and DNA methylation during embryonic stem cell derivation. *Cell J* 2018;20(3):361–368.
23. Xu RH, Sampsel-Barron TL, Gu F, et al. NANOG is a direct target of TGFbeta/actin-mediated SMAD signaling in human ESCs. *Cell Stem Cell* 2008;3(2):196–206.
24. Hannan NR, Jamshidi P, Pera MF, et al. BMP-11 and myostatin support undifferentiated growth of human embryonic stem cells in feeder-free cultures. *Cloning Stem Cells* 2009;11(3):427–435.
25. Faial T, Bernardo AS, Mendjan S, et al. Brachyury and SMAD signalling collaboratively orchestrate distinct mesoderm and endoderm gene regulatory networks in differentiating human embryonic stem cells. *Development* 2015;142(12):2121–2135.
26. Reubinoff BE, Pera MF, Fong CY, et al. Embryonic stem cell lines from human blastocysts: Somatic differentiation in vitro. *Nat Biotechnol* 2000;18(4):399–404.
27. Thomson JA, Itskovitz-Eldor J, Shapiro SS, et al. Embryonic stem cell lines derived from human blastocysts. *Science* 1998;282(5391):1145–1147.
28. van der Valk J, Brunner D, De Smet K, et al. Optimization of chemically defined cell culture media—Replacing fetal bovine serum in mammalian in vitro methods. *Toxicol In Vitro* 2010;24(4):1053–1063.
29. Ha SY, Jee BC, Suh CS, et al. Cryopreservation of human embryonic stem cells without the use of a programmable freezer. *Hum Reprod* 2005;20(7):1779–1785.
30. Llames S, Garcia-Perez E, Meana A, Larcher F, et al. Feeder layer cell actions and applications. *Tissue Eng Part B Rev* 2015;21(4):345–353.
31. Tannenbaum SE, Turetsky TT, Singer O, et al. Derivation of xeno-free and GMP-grade human embryonic stem cells—Platforms for future clinical applications. *PLoS One* 2012;7(6):e35325.
32. Aisenbrey EA, Murphy WL. Synthetic alternatives to Matrigel. *Nat Rev Mater* 2020;5(7):539–551.
33. Higuchi A, Kao SH, Ling QD, et al. Long-term xeno-free culture of human pluripotent stem cells on hydrogels with optimal elasticity. *Sci Rep* 2015;5:18136.
34. Holm F, Strom S, Inzunza J, et al. An effective serum- and xeno-free chemically defined freezing procedure for human embryonic and induced pluripotent stem cells. *Hum Reprod* 2010;25(5):1271–1279.
35. Zhang D, Mai Q, Li T, et al. Comparison of a xeno-free and serum-free culture system for human embryonic stem cells with conventional culture systems. *Stem Cell Res Ther* 2016;7(1):101.
36. Devito L, Jacquet L, Petrova A, et al. Generation of KCL034 clinical grade human embryonic stem cell line. *Stem Cell Res* 2016;16(1):184–188.
37. Ellerstrom C, Strehl R, Moya K, et al. Derivation of a xeno-free human embryonic stem cell line. *Stem Cells* 2006;24(10):2170–2176.
38. Tannenbaum SE, Singer O, Gil Y, et al. Hadassah, provider of “Regulatory-Ready” pluripotent clinical-grade stem cell banks. *Stem Cell Res* 2020;42:101670.
39. Ye J, Bates N, Soteriou D, et al. High quality clinical grade human embryonic stem cell lines derived from fresh discarded embryos. *Stem Cell Res Ther* 2017;8(1):128.
40. Barberi T, Willis LM, Socci ND, et al. Derivation of multipotent mesenchymal precursors from human embryonic stem cells. *PLoS Med* 2005;2(6):e161.
41. Gibson JD, O’Sullivan MB, Alaei F, et al. Regeneration of articular cartilage by human ESC-derived mesenchymal progenitors treated sequentially with BMP-2 and Wnt5a. *Stem Cells Transl Med* 2017;6(1):40–50.
42. Umeda K, Zhao J, Simmons P, et al. Human chondrogenic paraxial mesoderm, directed specification and prospective isolation from pluripotent stem cells. *Sci Rep* 2012;2:455.
43. Grogan SP, Dorthe EW, Glembotski NE, et al. Cartilage tissue engineering combining microspheroid building blocks and microneedle arrays. *Connect Tissue Res* 2020;61(2):229–243.
44. Martin I, Jakob M, Schafer D, et al. Quantitative analysis of gene expression in human articular cartilage from normal and osteoarthritic joints. *Osteoarthritis Cartilage* 2001;9(2):112–118.
45. Grogan SP, Barbero A, Winkelmann V, et al. Visual histological grading system for the evaluation of in vitro-generated neocartilage. *Tissue Eng* 2006;12(8):2141–2149.
46. Pineda S, Pollack A, Stevenson S, et al. A semiquantitative scale for histologic grading of articular cartilage repair. *Acta Anat (Basel)* 1992;143(4):335–340.
47. Crowe AR, Yue W. Semi-quantitative determination of protein expression using immunohistochemistry staining and analysis: An integrated protocol. *Bio Protoc* 2019;9(24):e3465.
48. Cleries R, Galvez J, Espino M, et al. BootstRatio: A web-based statistical analysis of fold-change in qPCR and RT-qPCR data using resampling methods. *Comput Biol Med* 2012;42(4):438–445.
49. DaCosta Byfield S, Major C, Laping NJ, et al. SB-505124 is a selective inhibitor of transforming growth factor-beta type I receptors ALK4, ALK5, and ALK7. *Mol Pharmacol* 2004;65(3):744–752.
50. Yan F, Wang Y, Wu X, et al. Nox4 and redox signaling mediate TGF-beta-induced endothelial cell apoptosis and phenotypic switch. *Cell Death Dis* 2014;5:e1010.
51. Dominici M, Le Blanc K, Mueller I, et al. Minimal criteria for defining multipotent mesenchymal stromal cells. The International Society for Cellular Therapy position statement. *Cytotherapy* 2006;8(4):315–317.
52. Studer D, Millan C, Ozturk E, et al. Molecular and biophysical mechanisms regulating hypertrophic differentiation in chondrocytes and mesenchymal stem cells. *Eur Cell Mater* 2012;24:118–135; discussion 135.
53. Abdel Mouti M, Pauklin S. TGFβ1/INHBA homodimer/nodal-SMAD2/3 signaling network: A pivotal molecular target in PDAC treatment. *Mol Ther* 2021;29(3):920–936.
54. Hertz S, Sawyer JS, Stauber AJ, et al. Clinical development of galunisertib (LY2157299 monohydrate), a small molecule inhibitor of transforming growth factor-beta signaling pathway. *Drug Des Devel Ther* 2015;9:4479–4499.
55. Kim BG, Malek E, Choi SH, et al. Novel therapies emerging in oncology to target the TGF-beta pathway. *J Hematol Oncol* 2021;14(1):55.

56. Wang J, Xiang H, Lu Y, et al. Role and clinical significance of TGFbeta1 and TGFbetaR1 in malignant tumors (review). *Int J Mol Med* 2021;47(4):55.
57. Kawata M, Mori D, Kanke K, et al. Simple and robust differentiation of human pluripotent stem cells toward chondrocytes by two small-molecule compounds. *Stem Cell Reports* 2019;13(3):530–544.
58. Wu T, Kamikawa YF, Donohoe ME. Brd4's bromodomains mediate histone H3 acetylation and chromatin remodeling in pluripotent cells through P300 and Brg1. *Cell Rep* 2018;25(7):1756–1771.
59. Wu T, Pinto HB, Kamikawa YF, et al. The BET family member BRD4 interacts with OCT4 and regulates pluripotency gene expression. *Stem Cell Reports* 2015; 4(3):390–403.

Address correspondence to:
Darryl D. D'Lima, MD, PhD
Shiley Center for Orthopaedic Research
and Education, at Scripps Clinic
10666 N Torrey Pines Road
La Jolla, CA 92037
USA

E-mail: ddlima@scripps.edu

Received: September 6, 2022
Accepted: November 15, 2022
Online Publication Date: January 31, 2023